Microfluidic sieve and detector for rapid ultrasensitive assays with single-molecule sensitivity

Geunyong Kim[1,2], Molly L. Shen[1,2], Andy Ng[1,2] and David Juncker[1,2*]

1. Biomedical Engineering Department, McGill University, Montreal, QC, Canada
2. Victor Phillip Dahdaleh Institute of Genomic Medicine, McGill University, Montreal, QC, Canada

The advent of ultrasensitive assays enabled many new research and clinical applications, but the time-to-result is hours and has not significantly improved over time, limiting their potential. We introduce the microfluidic sieve and detector (MSD) that can sieve 200 microlitres in just one minute, and quantify captured analytes in four minutes, down to zeptomolar (10^{-19}M) concentration. The MSD comprises half a million 8-µm-diameter pores that bind analytes upon Brownian motion-induced wall collision. Digital sandwich assays are completed by sequentially flowing the sample, reagents, partitioning the pores, and digitally revealing single 'trapped' analytes by enzymatic amplification. The MSD tests are specific and reproducible, exhibit a large dynamic range, and are easy-to-use, affordable, tuneable and versatile, enabling measurement of different proteins including influenza A nucleoprotein in clinical samples, and even nucleic acids while being both faster and more sensitive than PCR. As such, the MSD could open a new chapter for analysis and diagnostics.

Main

Rapid testing offers many advantages for diagnostics, but common approaches face trade-offs between sensitivity, time-to-result, simplicity and cost. Both protein and nucleic acid tests rely on binding between an analyte and a capture probe following their encounter upon diffusive, and sometimes convective, transport. Microfluidics has notably been used to shorten time-to-result by miniaturizing containers to speed-up diffusive mass transport[1-3]; however, this comes at the expense of sensitivity because the inclusion of a statistically representative number of analytes requires ever larger sample volumes, while microchannels only accommodate microscopic volumes. A strategy to both accommodate larger volumes yet minimize the time and distance of diffusive transport between analyte and probes is to disperse the latter in solution, either directly or attached to microparticles[4,5]. Nucleic acid tests[6-11] disperse probes and use complementary base pairing recognition to initiate exponential amplification (*e.g.* polymerase chain reaction and isothermal amplification) or collateral cleavage of reporter oligonucleotides in CRISPR-based tests, which enable ultrasensitive detection, but at a comparatively long time-to-result of tens of minutes for low concentrations, while being limited by a small volumetric capacity of typically a few microliters only. Protein immunoassays have historically been less sensitive and conventional enzyme-linked immunosorbent assays (ELISAs) only use linear amplification[12] and are lengthy. Ultrasensitive immunoassays are possible by using digital detection of single molecules in samples within oil-partitioned 'dead-end' microwells or droplets[13-17]. A breakthrough permitting robust, large volume processing was achieved by combining dispersed antibody-coated microparticles followed by partitioning them into microwells or droplets[18-22] or by direct flow cytometric counting[23] for digital detection; the microparticles capture and enrich analytes that are then sandwiched by detection antibody and enzyme for signal generation. However, the protocol remains lengthy (hours), and the instrumentation complex. Here we describe a microfluidic sieve and detector (MSD) that can sieve molecules very quickly using an isoporous membrane with each open-ended, micrometer-scale pore forming a Brownian affinity trap (BAT). Under commensurate sample flow, Brownian-motion induced wall collision leads to analyte capture within the BATs, which upon partitioning, turn into a digital detector array for quick counting and quantification of every 'trapped' analyte.

Results

The MSD test is completed by sieving the sample for 1 min, capturing analytes in BATs, and by detecting the captured analytes in 4 min via sandwich binding, then partitioning of each BAT into a closed compartment by oil capping and enzymatic conversion of a soluble substrate in each BAT, all within only 5 min, and achieves zM–aM–fM ultrahigh sensitivity and 7 OM dynamic ranges with good reproducibility of ≲15% coefficient of variation (CV), for both protein and nucleic acid analytes (Fig. 1a and see Figs. S1 and S2 in Supplementary Information for experimental setup and large-area MSD images with digital signals). In this study, the MSD comprised 500,000 BATs at a density of 800,000 pores cm^{-2} (40% open ratio) to permit rapid sieving of a sample at a high overall flow rate while meeting the commensurate, slow flow condition for a BAT, each of which is a cylindrical, open-ended micropore with a radius R_{BAT} = 4 μm and a length L_{BAT} = 20 μm (Fig. 1b,c). Akin to other digital assays, a single enzyme rapidly generates easily detectable fluorescence in the microscopic 1-pL BAT, thus permitting binary classification of BATs into positive ('1') and negative ('0'). As concentration increases, more BATs turn positive while the probability of more than one analyte per BAT also increases, which is predicted and compensated for by Poisson statistics and by calculating the average number of enzymes per BAT (AEB). For high percentage of positives (≳50%), AEB calculations become imprecise, but conversely analogue readout becomes possible simply by measuring the average fluorescence signal of the MSD (see method for signal readout details). By combining digital (MSD-D) and analogue (MSD-A) detection, the dynamic range of an MSD test can be extended[19]. Three critical features for MSD tests are (i) arrays of open-ended micropores (*i.e.* BATs) that are ~1,000 times larger than the sieved 'nanoparticles', facilitating clogging-free flow and affinity sieving, while minimizing the required pressure head, (ii) exclusive capture of analytes inside of the BATs, and not on the top and bottom surfaces between the BATs to preserve proportionality between number of molecules and positive counts, and (iii) leak-free capping with oil to partition BATs and enable digital readout.

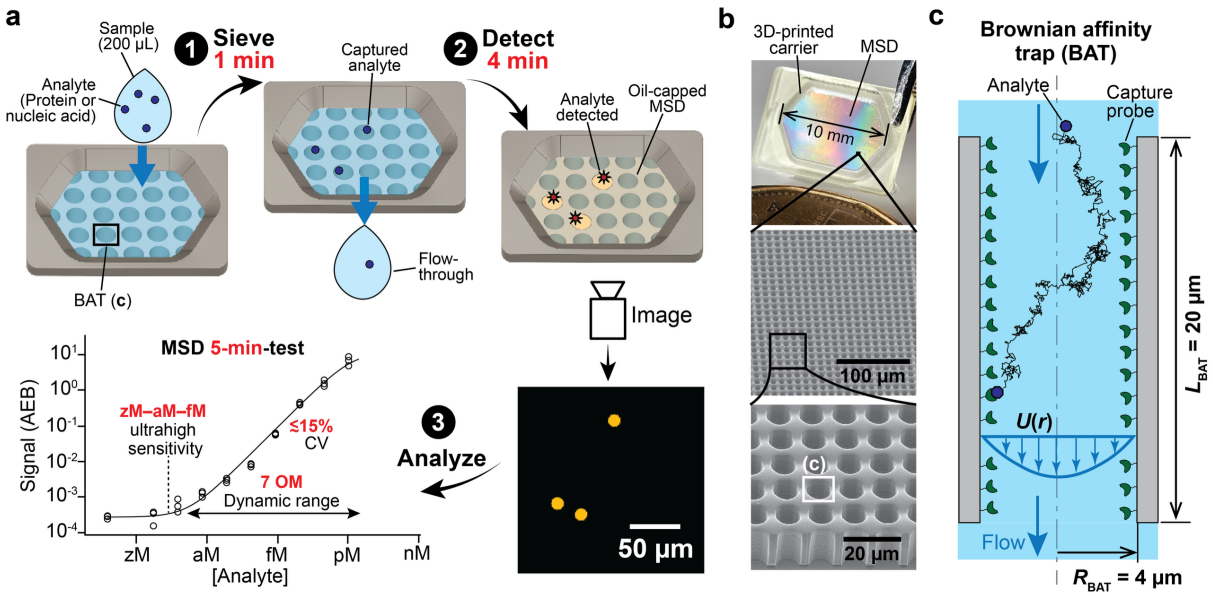

Fig. 1 | Microfluidic sieve and detector (MSD) made from an array of Brownian affinity traps (BATs) captures and detects single analytes in 5 min. a, MSD test procedure. The sample is sieved, reagents and buffers are sequentially flowed through the MSD, BATs are partitioned by oil capping, and BATs that contain one or more captured analytes become fluorescent upon enzymatic amplification, digitally revealing single molecule binding and realizing a rapid, ultrasensitive test. **b**, MSD with 500,000 BATs bonded to a 3D-printed carrier with successive magnification. **c**, Cross-section view of a 4 µm radius and 20 µm long BAT. A BAT is a microchannel coated with capture probe under commensurate flow promoting Brownian motion-induced wall collision of an analyte and affinity binding by the immobilized capture probe. The black trace reveals the path of a captured analyte.

Theoretical capture efficiency of the MSD and the BAT

A key metric of the MSD test is the analyte capture efficiency η of both the MSD and the BAT defined as the fraction of trapped to total analytes flowed through the MSD and BAT. We calculate η theoretically by ensemble (i) analytical and (ii) finite element method (FEM) calculations of binding reactions and by the (iii) stochastic Brownian agent dynamics (SBAD) we introduce. SBAD is a computational simulation of the Brownian motion of an analyte (the Brownian agent) as a random walk in the BAT under flow, while wall collision and affinity binding are simulated as stochastic events[24-26]. SBAD visualizes single analytes, is intuitive and accounts for the stochasticity and stochastic variance that are ignored by ensemble models, while accurate η are obtained by Monte Carlo estimation upon repeated simulations. We presume geometrical ergodicity implying that the η of a single BAT calculated by SBAD is equivalent to the η of a MSD,

and concentration ergodicity implying that ensemble calculations of the reaction η of a BAT as the concentration change from inlet to outlet is equivalent to the capture η of single molecules flowing through a BAT. For all models, we consider that analytes enter the BAT pore with a length L_{BAT} and a radius R_{BAT}, at an average flow velocity $\bar{U}$ following a parabolic Poiseuille flow profile and are subject to Brownian motion according to the diffusion coefficient D [m^2 s^{-1}], see Fig. 1c.

For the ensemble models, we consider the on-rate k_{on} [m^3 mol^{-1} s^{-1}] under first-order Langmuir kinetics, the surface density of the immobilized capture probe Γ [mol m^{-2}], and the surface-to-volume ratio $2/R_{BAT}$. We define $\kappa_{on} = 2k_{on}\Gamma/R_{BAT}$ [s^{-1}] as the effective on-rate and $\tau_{res} = L_{BAT}/\bar{U}$ [s] as the average residence time of the sample. In this study, we operate under conditions of large κ_{on} (~10^{-1}–10^2 s^{-1}), low density of bound analyte, and short timescales with low off-rates k_{off} (~10^{-6} s^{-1}), so that dissociation can be neglected in the analysis. The Péclet (Pe) and Graetz (Gz) numbers quantify the ratio of convective to diffusive transport and are > 1 for all experiments, indicating convection-dominated transport. Damköhler numbers (Da) express the ratio of the reaction to mass transport rates and we consider the first Damköhler number, $\mathrm{Da_I} = \kappa_{on}\tau_{res}$ representing the ratio of reaction rate to convective mass transport and a surface Damköhler number, $\mathrm{Da_s} = k_{on}\Gamma/k_c$ with k_c [m s^{-1}] being the mass transfer coefficient used in thin film theory, and which is the ratio of reaction rate to the total mass transport to the surface including both convection and diffusion (Fig. S3 and Supplementary Information)[1,27,28]. We calculate the ensemble reaction efficiency η of a BAT following classical derivations[28-30] and find (Fig. S4 and Supplementary Information for the detailed derivation):

$$\eta = 1 - e^{\frac{-\mathrm{Da_I}}{1+\mathrm{Da_s}}} \tag{1}$$

For all experiments in this study, $\mathrm{Da_s} < 1$, hence we obtain:

$$\eta = 1 - e^{-\mathrm{Da_I}} \tag{2}$$

Hence, η is adjustable by varying κ_{on} (*e.g.* via the surface density of capture probes) and τ_{res} via $\bar{U}$. The FEM ensemble calculations directly solve the coupled convection-diffusion-reaction equations without simplifying assumptions and provide spatially resolved concentration fields, from which η is obtained as the ratio of the outlet to inlet average concentration, Fig. 2a,b.

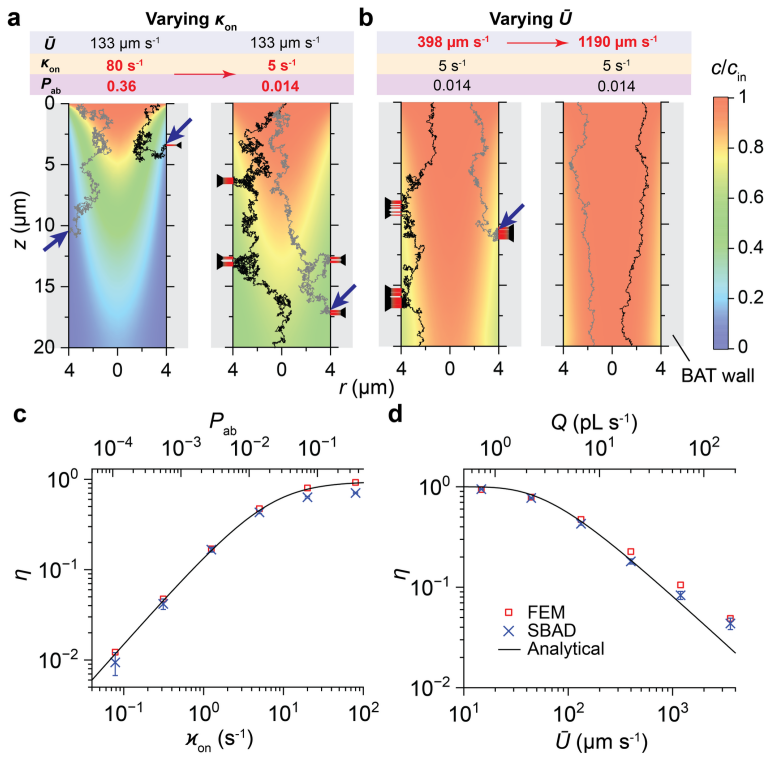

Fig. 2 | Stochastic Brownian agent dynamics (SBAD) traces and analytical, SBAD and FEM calculations of BAT capture efficiency η for different conditions. a, SBAD example traces overlaid on FEM simulation for a model 100 kDa globular protein analyte with a diffusion coefficient $D = 80$ μm^2 s^{-1} with varying effective on-rate κ_{on} and affinity binding probability P_{ab} at a fixed average flow speed, $\bar{U} = 133$ μm s^{-1}, and with **b**, varying $\bar{U}$ at fixed $\kappa_{on} = 5$ s^{-1} and $P_{ab} = 0.014$. Arrows record analyte binding while red bars with a black arrow tail indicate wall collision without binding. The colour bar indicates the ratio, c/c_{in}, where c is the local analyte concentration and c_{in} is the inlet concentration. **c**, η as a function of κ_{on} at $\bar{U} = 133$ μm s^{-1} and **d**, of $\bar{U}$ at $\kappa_{on} = 5$ s^{-1}. SBAD error bars represent the two-sided 95% confidence interval of SBAD with $N = 5{,}000$ and increase for low η due to stochastic noise.

SBAD analysis is described in detail in Supplementary Information including the computational algorithm in Fig. S5. Example traces visualizing random-walk analyte trajectories under different flow conditions and varying surface affinity, are shown as slow-motion, time-stamped animations in Supplementary Videos S1–S3, and as traces superposed with FEM ensemble models of concentration in Fig. 2a,b. To calibrate SBAD, we introduce the affinity binding probability upon wall collision (P_{ab}) as a free parameter. Benchmarking against η obtained from the FEM calculations, calibration was performed for the model system with a 100 kDa globular protein analyte with $D = 80$ μm^2 s^{-1} flowing at $\bar{U} = 10$ μm s^{-1}. P_{ab} was determined and

found to be proportional to κ_{on} (Fig. S6 and Supplementary Information) for a wide range of κ_{on}, and constant relative to τ_{res} (and $\bar{U}$) across a broad range, Fig. 2c,d. A lower κ_{on} (and lower P_{ab}) result in a higher number of non-binding collisions, and a lower τ_{res} in fewer wall collisions, both contributing to lower η. The calibrated SBAD was consistent with both FEM and analytical calculations while capturing stochastic variances of single-analyte binding in BATs.

MSD membrane manufacturing and functionalization

MSDs were made by moulding and photopolymerization of a perfluoropolymer forming an isoporous membrane almost identical to the one used for size-exclusion-based filtration of circulating tumour cells[31,32], but used here for Brownian affinity trapping of molecular analytes inside of the pores. A crucial prerequisite for MSD assays is two-sided hydrophobicity of the membrane to both prevent unwanted binding of the analytes on the 'top surface', outside of the BAT, which could confound assay results, and to form a water-tight seal upon capping with fluorinated oil and partition each BAT for digital assay readout. We developed float-flip-float process to exclusively functionalize the inside of BATs with capture probes and preserve hydrophobicity on the top and bottom surfaces of MSDs as described in Supplementary Information and shown in Fig. S7.

Experimental efficiency of the MSD and of the BAT

We systematically evaluated MSD and BAT sieving η experimentally with an array of 500,000 BATs. The captured analytes were directly detected via a one-step MSD test, Fig. 3a; see Supplementary Information and Fig. S1 for experimental details. Briefly, MSDs were functionalized with biotin as a capture probe, and streptavidin-β-galactosidase conjugate (SβG) was used as a combined "analyte-detection probe-enzyme". The direct detection of the captured analytes eliminates confounding factors arising from downstream steps such as detection probe and enzyme incubations that contribute to false positives and negatives. We independently established κ_{on} = 7.44 s^{-1} and P_{ab} = 0.035 with high density functionalization (for details on κ_{on}, see Figs. S8 and S9, and Table S1 in Supplementary Information).

In typical experiments, 200-μL-samples were sieved at a flow velocity of $\bar{U}$ = 133 μm s^{-1} for 1 min and the captured molecules were detected following sequential 1-min steps of washing and flowing of resorufin-β-D-galactopyranoside (RGP), followed by oil capping and enzymatic

conversion of RGP into fluorescent resorufin. We evaluated the number of captured molecules as a function of the volume over 2 OM and observed the expected proportionality, Fig. 3b. The MSD and BAT efficiency η was quantified by calculating the ratio of captured to total number of molecules flowed under varying conditions, and compared to theory. We varied flow velocity (and corresponding flow rate) and κ_{on} (and corresponding P_{ab}) over at least 2 OM each. κ_{on} was modulated by varying the surface density of biotin serving as the capture probe by ratiometric incorporation of spacer molecules and via different capture probe types. We compared experimental results with analytical, FEM and SBAD predictions, and found strong concordance in all cases, Fig. 3c,d, thus mutually validating and reinforcing theory (notably SBAD analysis) and experimental findings. The data showcase rapid, predictable and tuneable analyte capture by microfluidic sieving of 200 µL in just 2 s with $\bar{U}$ = 3,580 µm s^{-1} for η ~ 2% (characteristic convection time 10^{-3} s << reaction time ~10^{-1} s < characteristic diffusion time ~ 1 s), and in 1 min with $\bar{U}$ = 133 µm s^{-1} for η ~ 50% (with similar characteristic convection and reaction times of ~10^{-1} s), for diverse capture probes including biotin, antibodies and nucleic acids, and with linearly increasing numbers with volume.

Next we evaluated how a high η ~ 50% could benefit assay performance for the one-step test by establishing a standard binding curve for varying concentrations of SβG. We used dynamic thresholding to distinguish positive and negative BATs that proved robust with a coefficient of variation (CV) of 9%, but with residual false-positives (AEB ~10^{-4}) at zero concentration, Fig. 3e. Both the stochastic analyte capture with its standard error (that can be evaluated using the SBAD simulation), and stochastic sampling with Poisson noise, each leading to increased fluctuations scaling with the square root, contribute to CV and become significant for low analyte numbers. The overall noise fluctuated from 40% below the limit of detection (LOD) to 11% in the linear range, which we consider to be good for a manual test. The readout accuracy drops for AEB > 0.5 because increasing number of BATs will have more than one analyte, and for test results above this threshold average fluorescence signals are quantified by MSD-A readout. With the combined MSD-D and MSD-A, we obtained an LOD of 35.9 zM and a linear dynamic range of ~7 OM for a 4-min-test, which is remarkable.

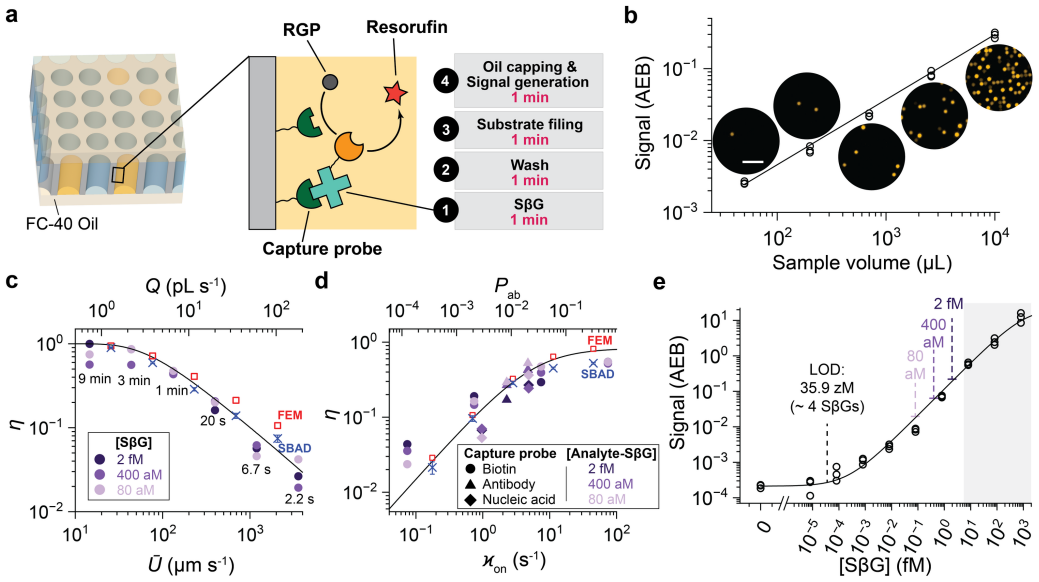

Fig. 3 | Experimental one-step MSD test sieving efficiency η is concordant with theory. MSD tests were conducted using a 200 μL solution containing streptavidin-β-galactosidase (SβG, MW = 530 kDa and D = 45.9 μm^2 s^{-1}) flowed through an array of 500,000 BATs in 1 min with $\bar{U}$ = 133 μm s^{-1} and with κ_{on} = 7.44 s^{-1}, unless indicated otherwise. **a**, Workflow of one-step MSD test with SβG "analyte-detection probe-enzyme". **b**, The number of captured analytes (i.e., AEB) as function of sample volume follows a linear relationship with a slope of 0.91 and R^2 = 0.99. Insets are illustrative MSD images. Scale bar = 50 μm. **c**, Experimental sieving efficiency η as a function of flow speed $\bar{U}$ (and corresponding flow rate Q and incubation times) and **d**, of κ_{on} (and corresponding P_{ab}) for different capture probes (biotin, antibody, nucleic acid each with its corresponding analyte-SβG system) and varying surface density. η was measured for analyte concentration of 2 fM, 400 aM and 80 aM, and found to be invariable as expected. Line is analytical model, squares are FEM and '×' is SBAD. **e**, MSD standard binding curve for this 4-min test (see **a**). The white and greyed areas of the curve correspond to MSD-D and MSD-A, respectively. The limit of detection (LOD) was defined as the concentration yielding an AEB equal to the mean of the zero-concentration sample plus three standard deviations, accounting for both experimental and Poisson noise.

Sandwich MSD test for protein quantification and influenza A virus detection from nasopharyngeal swab samples

We extended MSD tests to sandwich assays for proteins with a time-to-result of 5 min accounting for capture and digital detection of molecules. Similar to a conventional ELISA, the sandwich MSD test is based on sequentially introducing the sample containing the analyte, biotinylated detection antibody and the streptavidin-enzyme conjugate (*i.e.* SβG in our case), leading to an enzymatic sandwich complex, which then produces fluorescent resorufin from RGP

(see Fig. 4a,b and Fig. S1 in Supplementary Information). The sandwich format introduces additional sources of noise, and most significantly the non-specific binding of either the detection probe or of SβG each contribute to false positive BATs. False positives quickly degrade assay sensitivity and performance, and should be kept low[20]. We thus systematically optimized blocking, reagent concentration, flow time, flow speed to reach a background signal for negative controls of ~2×10^{-3} AEB, *i.e.* ~1,000 positive BATs for an MSD with 500,000 BATs. Standard curves for IL-4 and influenza A nucleoprotein were generated with the 5-min MSD test and with a classical 4-h ELISA in microplates, Fig. 4c,d. The LODs of the ELISA were 118 fM (1.77 pg ml^{-1}) and 918 fM (52.1 pg ml^{-1}), respectively, and of the MSD 325 aM (4.88 fg ml^{-1}) and 2.00 fM (113 fg ml^{-1}), respectively. The dynamic ranges were ~ 2 OM for the ELISA, and 7 OM for the combined MSD-D and MSD-A. The MSD was thus 50 times faster and ~350 times more sensitive, and dynamic range was extended not only at the low, but also at the high concentration range by 2–3 OM *vs* ELISA. The LOD and CVs of the MSD test are similar or better compared to other ultrasensitive assays, but with a time-to-result of only 5 min *vs* 2–4 h[18-22].

To evaluate the potential of the MSD for clinical translation, we tested 15 influenza A-positive and 15 negative samples obtained via nasopharyngeal swabbing and diagnosed using RT-qPCR (See Table S2 for demographics), and compared it to a commercial rapid test. Influenza A nucleoprotein was released by adding lysis buffer and waiting for 5 min, and measured using both the 15-min rapid test and the 5-min MSD test (Fig. 4e). The rapid test detected 6 out of 15 positives (Fig. S10), yielding 40% sensitivity (95% CI, 20–64%), and 100% specificity (95% CI, 80–100%). The MSD test detected all positives including those missed by the rapid test, with one false positive (Fig. 4f), yielding 100% sensitivity (95% CI, 80–100%) and 93% specificity (95% CI, 70–99%; see Fig. 4g,h for confusion matrices of both tests). Receiver operating characteristic (ROC) curve yielded an area under the curve (AUC) of 0.98 and 0.83 for the MSD and rapid test (Fig. 4i), respectively. In this small cohort, the MSD test expectedly outperformed rapid tests while matching PCR sensitivity. Larger cohorts and further investigation will be needed to accurately benchmark MSD tests. These results illustrate the potential of the MSD as a rapid, ultrasensitive diagnostic test. The intrinsic sensitivity of the MSD suggests a potential for improved diagnostic sensitivity compared to PCR when considering that there are ~530 nucleoproteins for 1 genetic copy per influenza A virus.

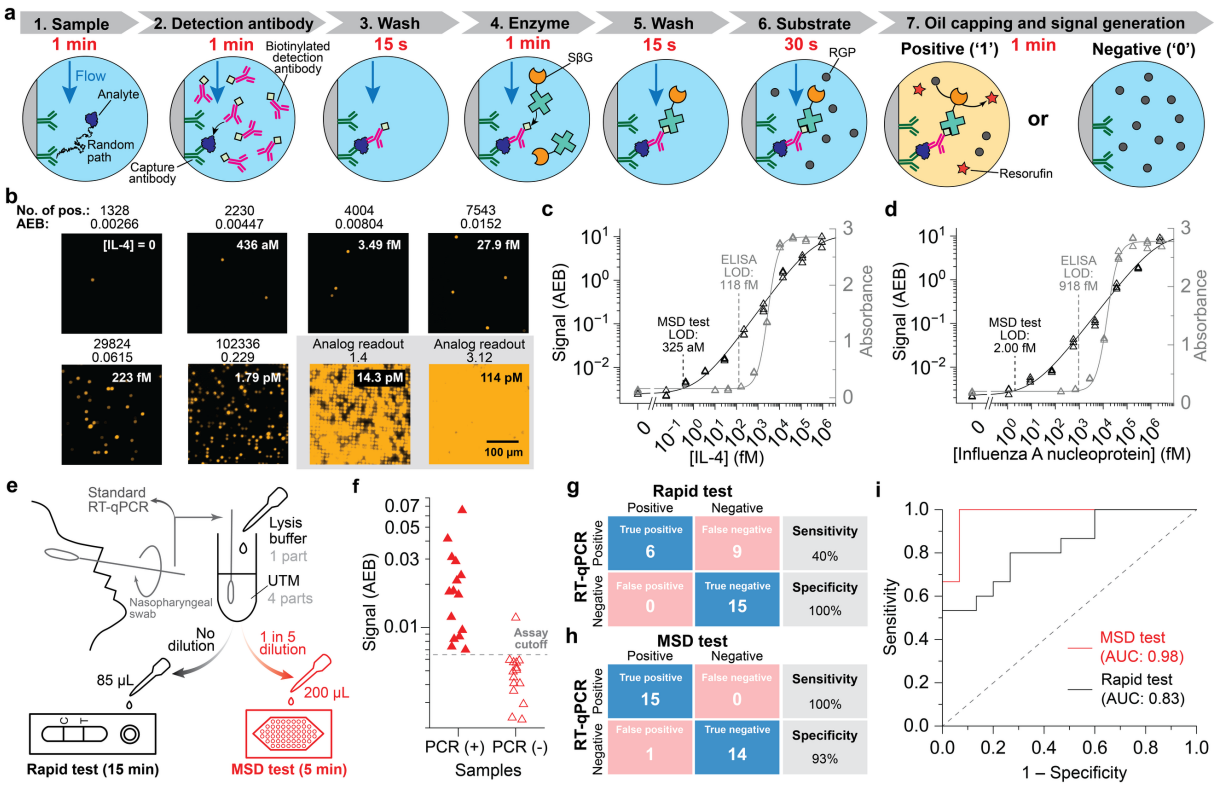

Fig. 4 | Sandwich MSD for protein detection and its application to influenza A detection from nasopharyngeal swab samples. a, 5-min MSD test based on a sandwich immunoassay workflow. The sample with the analyte, biotinylated detection antibody, enzyme conjugate, substrate and wash buffers are flowed sequentially for the indicated duration, followed by oil capping of the BATs, signal generation and quantification. **b**, Fluorescence images of the MSD test against IL-4 with concentrations, positive counts and quantification by calculating the average number of enzymes per BAT (AEB). Quantification is achieved by digital counting (MSD-D) from ultralow to low concentrations, and by the average signal of the MSD (MSD-A) for higher concentrations (greyed area), thereby extending the dynamic range of the test. **c**, Standard curves of 5-min MSD test for IL-4 and **d**, for influenza A virus nucleoprotein. The standard curves from MSD test and the benchmark microplate ELISA are shown in black and grey, respectively. The coefficients of variation (CVs) for IL-4 and influenza A nucleoprotein are 14 and 12 %, respectively. All LODs were defined as the concentrations yielding an AEB three standard deviations above the mean AEB of the zero-concentration sample. **e,** Influenza A detection from nasopharyngeal swab samples. Nasopharyngeal swab samples in universal transport medium (UTM) were lysed to release influenza A virus nucleoprotein. The samples were then tested by both a 15-min rapid test without dilution and the 5-min MSD test after a 5-fold dilution. **f**, MSD test results of 15 positive and 15 negative samples. **g**, Confusion matrices for the rapid test and **h**, for the MSD test. **i**, Receiver operating characteristic (ROC) curves for the rapid test and MSD test. Areas under the curve (AUCs) for the rapid test and MSD test were evaluated as 0.83 and 0.98, respectively.

Sandwich MSD test for nucleic acid detection with sensitivity competitive with PCR

We reasoned that the MSD test could be used for nucleic acid detection. We selected miR-141 as the target analyte because it is small and compatible with sandwich-based detection needed for SβG binding and enzymatic amplification (Fig. 5a), and compared it to polymerase chain reaction (PCR), which serves as a gold standard. The LOD of the MSD tests was 7.05 fM for a 200 μL sample, again with a 5 min time-to-result (Fig. 5b) which we found to rival the LOD of reverse-transcription quantitative PCR (RT-qPCR) that was 1.93 fM at the background cycle threshold (Ct) of 35. However, PCR lasted for 2h and operated from ~ 1 μL of effective sample volume (Fig. S11). Droplet digital PCR (ddPCR) was evaluated but did not outperform the MSD test; inefficient reverse transcription (RT) and numerous false-positive droplets caused by carryover of the RT primer limited sensitivity, failing detection of miR-141 even at 240 fM (data not shown). The MSD test illustrates that linear enzymatic signal amplification in a microscopic volume (1 pL) with a high turnover rate (~10^3 s^{-1} for βG[33]) can detect molecules in < 1 min, thus outperforming the exponential amplification of PCR by thermocycling. PCR is further limited to ~1 μL and a separate pre-concentration is required to increase sensitivity, while MSD sensitivity can be improved by sieving larger volumes, here with up to 5 mL for 25 min sieving at the same flow rate and an improved LOD of 206 aM (Fig. 5c). The MSD test compares favourably to PCR with its simpler protocol and instrumentation, shorter time-to-result, and improved LOD with larger volumes.

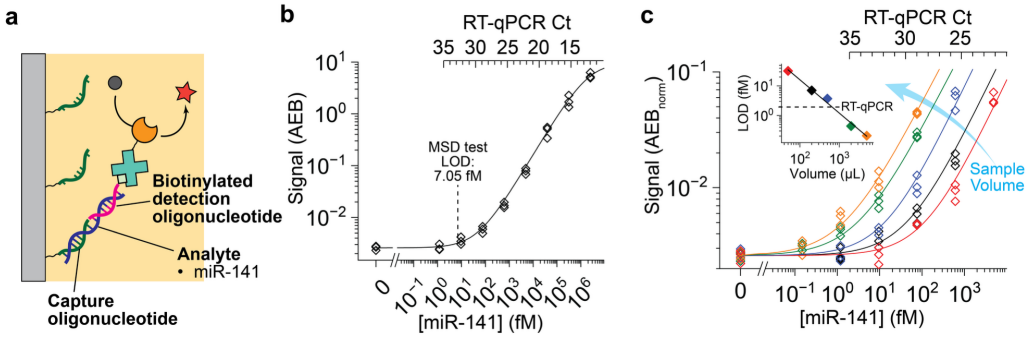

Fig. 5 | MSD test detects nucleic acid via sandwich binding much faster than PCR, and is increasingly more sensitive with larger volumes. a, Sandwich complex for nucleic acid detections. **b**, Standard curve of 5-min MSD test for miR-141. The CV is 17%. **c**, Standard curves for volumes of 50 μL (red), 200 μL (black, reference), 500 μL (blue), 2 mL (green) and 5 mL (orange). All samples were flowed at 200 μL min^{-1} followed by the 4 min detection, resulting in total assay times of 4.25, 5, 6.5, 14 and 29 min, respectively. The inset

shows LODs for varying sample volumes and corresponding LOD for RT-qPCR as dashed line. All LODs were defined as the concentrations yielding an AEB three standard deviations above the mean AEB of the zero-concentration sample.

Discussion

The MSD test uses microfluidic sieving to capture proteins and nucleic acids in 200 µL in one minute with 50% efficiency, and then count individual captured molecules in four more minutes via a ternary sandwich assay and digital detection within partitioned BATs. The capture efficiency η is predictable and tuneable based on flow rates and effective on-rates (κ_{on}), and was confirmed by the proposed SBAD, ensemble analytical and FEM calculation, and experiments. ~50% of molecules in a 200-µL-sample could be captured in just 1 min sieving with 500,000 BATs at $Da_I \sim 1$ and $Da_s < 1$. Conventional macroscopic sieves rely on size-exclusion with pores smaller than the filtrate and are susceptible to clogging and caking, while in molecular sieves pore and molecule size are commensurate[34]. In contrast, in microfluidic sieving introduced here the diameter of the pores (i.e. the BATs) is >1,000 times larger than target analytes, which supports sample flow with hardly any pressure required while simultaneously minimizing the risk of clogging. The MSD showcases the hitherto untapped potential of vertical flow-through in sensor design that enables rapid capture, and together with partitioning and fast enzymatic signal amplification, make for an overall fast and ultrasensitive test (zeptomolar for a model system), and endow it with a broad dynamic range of seven orders of magnitude and a low CV suitable for quantification. Hence, it improves on the time-to-result of common single molecule immunoassays by well over an order of magnitude, and simultaneously becomes an alternative for nucleic acid detection because it is faster than common nucleic acid tests, and more sensitive with increasing volume, Fig. 6.

In this study, we presented the MSD and its rapid, efficient capture of analytes, and ultrasensitive, *in situ* digital (and analogue) detection in five minutes based on a large array of BATs. The MSD recasts the trade-off of speed *vs* sensitivity from hours and pM to minutes and aM, all while being simple, highly specific thanks to the sandwich assay configuration and adaptable, thus unlocking amplification-free nucleic acid testing. The MSD is a thin, isoporous polymer membrane and is predisposed for integration and for automation thanks to a flow through protocol, and open to future improvements. The MSD test, with single molecule sensitivity, short time-to-result, large dynamic and volumetric range, affordability, ease of use, and versatility has

the potential to redefine the rules of diagnostics and analysis and open multiple new opportunities and applications.

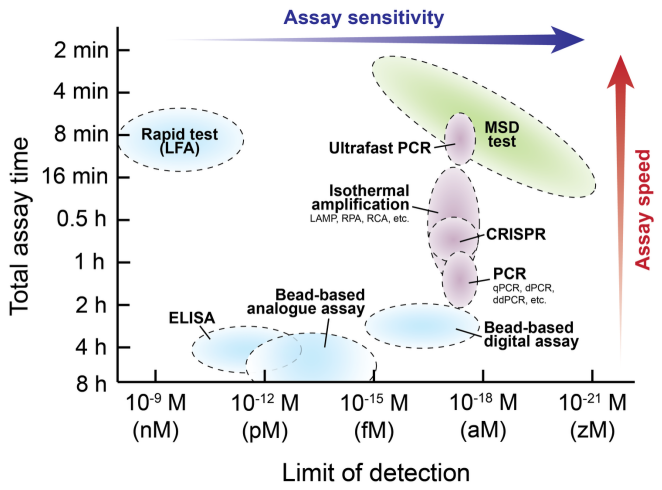

Fig. 6 | MSD test benchmarking. The LODs and total assay times of protein assays[4,5,18-23,35] including ELISA, rapid tests, bead-based analogue and digital assays are shown in blue while nucleic acid amplification tests[11] including PCR, isothermal amplification, and CRISPR-based detection are shown in purple. The current MSD test is shown as a slanted green oval reflecting its tuneability and trade-off between improving sensitivity further by flowing larger volumes *vs* longer time-to-result.

Materials and methods

Materials

Microfluidic sieve and detector (MSD) fabrication

Fluorolink MD 700 (Lot #BL2718, Solvay Specialty Polymers USA LLC, Alpharetta, GA, USA), 2-Hydroxy-2-methylpropiophenone (Darocur 1173) (Cat. #405655, lot #MKCD9390, Sigma-Aldrich, Oakville, ON, Canada), Ebecryl® 3708 (Cat. #024709A, lot #NA0275104, Allnex Canada Inc., Ottawa, ON, Canada), Tripropylene glycol diacrylate (TPGDA) (Cat. #027600A, lot #NA0073085, Allnex Canada Inc., Ottawa, ON, Canada), 3,4-Epoxycyclohexylmethyl 3,4-epoxycyclohexanecarboxylate (Cat. #407208, lot #MKCP6704, Sigma-Aldrich, Oakville, ON, Canada), Capa® 3050 (Lot #0000001917, Ingevity UK Ltd, Warrington, Cheshire, UK), Uvacure 1600 (Cat. #028382A, lot #SE103117, Allnex Canada Inc., Ottawa, ON, Canada), Poly(ethylene glycol) diacrylate (PEGDA)-250 (Cat. #475629, lot #MKCS0144, Sigma-Aldrich, Oakville, ON, Canada), diphenyl(2,4,6-trimethylbenzoyl)phosphine oxide (TPO) (Cat. #415952, lot #MKCS4625, Sigma-Aldrich, Oakville, ON, Canada), 2-isopropylthioxanthone (ITX) (Cat. #I067825G, lot #XJHJH-LA, TCI America, Portland, OR, USA), pentaerythritol tetraacrylate (PETTA) (Cat. #408263, lot #MKCR5556, Sigma-Aldrich, Oakville, ON, Canada).

MSD functionalization

N-Acryloxysuccinimide (NAS; Acrylic acid N-Hydroxysuccinimide (NHS) ester) (Cat. #S0814, lot #8QMTA-WX, TCI America, Portland, OR, USA), TPO, Darocur 1173, Dimethyl sulfoxide (DMSO) (Cat. #036480.K2, lot #X11K026, Thermo Fisher Scientific, Waltham, MA, USA), 1H,1H-Heptafluorobutylamine (Cat. #H1300, lot # EMNAH-IR, TCI America, Portland, OR, USA), Biotin-PEG7-amine (Cat. #BP-21622, lot #B103-085, Broadpharm, San Diego, CA, USA), m-PEG2-amine (Cat. #BP-21109, lot #20230322A, Broadpharm, San Diego, CA, USA), Anti-βG (Cat. #Z3783, lot #0000628031, Promega, Madison, WI, USA), Purified anti-streptavidin (Cat. #410501, lot #B294133, Biolegend, San Diego, CA, USA), Capture DNA oligonucleotide for BAT efficiency measurement (5'- /5AmMC12/CAC GCA TCA CCA -3', Integrated DNA Technologies, Coralville, IA, USA), miR-141 capture oligonucleotide (5'- /5AmMC12/TTT TTT TTC +CAT CT+T TA+C +C -3', Integrated DNA Technologies, Coralville, IA, USA), Purified anti-human IL-4 (Cat. #500702, lot #B372341, Biolegend, San Diego, CA, USA), Influenza A virus Nucleoprotein antibody (Cat. #GTX41278, lot #822305152, GeneTex, Irvine, CA, USA).

Streptavidin-β-galactosidase (SβG) conjugation

Streptavidin protein (Cat. #21122, lot #ZA379579, Thermo Fisher Scientific, Waltham, MA, USA), β-Galactosidase from *Escherichia coli* (Cat. #G5635, lot #0000286885, Sigma-Aldrich, Oakville, ON, Canada), TCO-PEG4-NHS ester (Cat. #BP-22418, lot #B154-066, Broadpharm, San Diego, CA, USA), Methyltetrazine-PEG4-NHS ester (Cat. #BP-22945, lot #B143-046, Broadpharm, San Diego, CA, USA), Glycerol (Cat. #BP229-1, lot #151821, Thermo Fisher Scientific, Waltham, MA, USA).

MSD test for SβG, IL-4, Influenza A nucleoprotein and miR-141

Biotinylated DNA oligonucleotide analyte (5'- /5BiotinTEG/TGG TGA TGC GTG -3', Integrated DNA Technologies, Coralville, IA, USA), Biotinylated DNA oligonucleotide analyte with double mismatch (5'- /5BiotinTEG/TGG TGT AGC GTG -3', Integrated DNA Technologies, Coralville, IA, USA), miR-141 (5'- rUrArA rCrArC rUrGrU rCrUrG rGrUrA rArArG rArUrG rG -3', Integrated DNA Technologies, Coralville, IA, USA), Biotinylated miR-141 detection oligonucleotide (5'- +A+GA +CA+G TG+T TA/3Bio/ -3', Integrated DNA Technologies, Coralville, IA, USA), Recombinant Human IL-4 Protein (Cat. #204-IL-010/CF, lot #NCL0723062, R&D Systems, Minneapolis, MN, USA), Biotin anti-human IL-4 (Cat. #500804, lot #B360555, Biolegend, San Diego, CA, USA), Influenza A H1N1 (A/Puerto Rico/8/34/Mount Sinai) Nucleoprotein (Cat. #11675-V08B, lot #LC16MY3024, Sino Biological, Wayne, PA, USA), Anti-H7N9 Nucleoprotein (Cat. #11675-R705, lot #HA12DE0602, Sino Biological, Wayne, PA, USA), Resorufin β-D-Galactopyranoside (RGP) (Cat. #R1159, lot #2647827, Thermo Fisher Scientific, Waltham, MA, USA), Fluorinert™ FC-40 (Cat. #F9755, lot #MKCF9430, Sigma-Aldrich, Oakville, ON, Canada), Tris base (Cat. #648311, lot #3782098, Sigma-Aldrich, Oakville, ON, Canada), Sodium chloride (NaCl) (Cat. #S271-500, lot #223105, Thermo Fisher Scientific, Waltham, MA, USA), Magnesium chloride ($MgCl_2$) (Cat. #012315.A1, lot #N22J024, Thermo Fisher Scientific, Waltham, MA, USA), PBS 10x (Cat. #70011-044, lot #3048030, Thermo Fisher Scientific, Waltham, MA, USA), Tween-20 (Cat. #P7949, lot #SLBX0835, Sigma-Aldrich, Oakville, ON, Canada), SuperBlock™ Blocking Buffer (Cat. #37516, lot #AA403418, Thermo Fisher Scientific, Waltham, MA, USA), Nuclease-free water (Cat. #W4502, lot #0000344156, Sigma-Aldrich, Oakville, ON, Canada).

Benchmarking RT-qPCR, ddPCR and ELISA

miR-141, TaqMan™ MicroRNA Reverse Transcription Kit (Cat. #4366596, lot #3083491, Thermo Fisher Scientific, Waltham, MA, USA), TaqMan™ MicroRNA Assay (Cat. #4427975, lot #P241216, Thermo Fisher Scientific, Waltham, MA, USA), TaqMan™ Universal Master Mix II, with UNG (Cat. #4440042, lot #3006006, Thermo Fisher Scientific, Waltham, MA, USA), QX200™ droplet generation oil (Cat. #1864005, lot #L006641, Bio-Rad, Hercules, CA, USA), ddPCR™ Supermix for Probes (Cat. #186-3026, lot #64673787, Bio-Rad, Hercules, CA, USA), DG8™ Cartridges for QX200™ Droplet Generator (Cat. #1864008, lot #1000125499, Bio-Rad, Hercules, CA, USA), Nunc™ MaxiSorp™ ELISA Plates, Uncoated (Cat. #423501, lot #B447813, Biolegend, San Diego, CA, USA), Purified anti-human IL-4, Biotin anti-human IL-4, Recombinant Human IL-4 Protein, Influenza A virus Nucleoprotein antibody, Anti-H7N9 Nucleoprotein, Influenza A H1N1 (A/Puerto Rico/8/34/Mount Sinai) Nucleoprotein, Pierce™ High Sensitivity Streptavidin-HRP (Cat. #21130, lot #YE375674, Thermo Fisher Scientific, Waltham, MA, USA), 3,3',5,5'-Tetramethylbenzidine (TMB) (Cat. #T8665, lot #059K5307, Sigma-Aldrich, Oakville, ON, Canada), Sulfuric acid (H_2SO_4) (Cat. #351293-500, lot #115107, Thermo Fisher Scientific, Waltham, MA, USA), Sodium bicarbonate ($NaHCO_3$) (Cat. #S233-500, lot #071014, Thermo Fisher Scientific, Waltham, MA, USA), Sodium carbonate (Na_2CO_3) (Cat. #S7795, lot #SLBT9993, Sigma-Aldrich, Oakville, ON, Canada), PBS 10x, Tween-20, Bovine serum albumin (BSA) (Cat. #001-000-162, lot #172667, Jackson ImmunoResearch, West Grove, PA, USA).

Influenza patient sample analysis

Influenza nasopharyngeal swab samples (American Blood Services DBA, Los Osos, CA, USA), Tris Base, NaCl, DTT (Cat. #R0861, lot #3047435, Thermo Fisher Scientific, Waltham, MA, USA), Halt™ Protease Inhibitor Cocktail (Cat. #78430, lot #3213813, Thermo Fisher Scientific, Waltham, MA, USA), RNase A (Cat. #EN0531, lot #3250577, Thermo Fisher Scientific, Waltham, MA, USA), Glycerol, Triton X-100 (Cat. #BP151-500, lot #051126, Thermo Fisher Scientific, Waltham, MA, USA), Influenza AB + COVID-19 Antigen – 3 in 1 Test (Cat. #COF-19CPC25, lot #I2410155, BTNX Inc., Pickering, ON, Canada).

Methods

Stochastic Brownian agent dynamics (SBAD) and finite element method (FEM) simulations

Stochastic Brownian agent dynamics (SBAD) operating the flow chart in Fig. S5 was developed on MATLAB v.R2024a (Mathworks, Natick, MA, USA). For a model 100 kDa globular protein analyte, the diffusion coefficient D = 80 μm^2 s^{-1}, was estimated by the Stokes-Einstein-Sutherland equation. SBAD was carried out with Monte Carlo methods, for a high number of analytes to obtain the efficiency η. FEM using COMSOL Multiphysics v.6.3 (COMSOL, Inc., Burlington, MA, USA) was employed to obtain ensemble solution of analyte capture in a BAT while varying κ_{on} and $\bar{U}$. The efficiencies η were obtained from the integrated concentration on the inlet and outlet plane of a BAT. Based on concentration ergodicity, binding probability P_{ab} in SBAD was calibrated by benchmarking against the FEM ensemble solutions (See Supplementary Information for details).

Fabrication and functionalization of MSDs

4 × 4 cm^2 membranes with vertical, 8-μm diameter and 20-μm long pores in a rectangular array of a 40 % open ratio were fabricated with MD 700 by moulding as detailed in our previous publication[31] and the isoporous membrane was used as an MSD. Scanning electron microscope (SEM) images of the isoporous membrane were collected on a FEI Quanta 450 environmental scanning electron microscope (FE-ESEM). To fabricate MSDs with 500,000 BATs on a 3D-printed carrier shown in Fig. 1b, the membranes were cut into 1.3 × 1 cm^2 pieces, and attached to a carriers 3D-printed with PEGDA-based ink (PLInk)[36] by using uncured PLInk as a glue to bond the membrane piece and the carrier upon UV exposure. To ensure that the top and bottom surfaces of the MSDs remained free of capture probe and hydrophobic, the MSDs were functionalized by the float-flip-float method (Fig. S7). First, for NHS-activation, the MSDs were floated top side-up on 100 mM acrylic acid NHS ester with 10 mM TPO and 2 % (v/v) Darocur 1173 in DMSO, and exposed to UV using a UV Chamber (IntelliRay 600, Uvitron International, Inc., West Springfield, MA, USA) at 70 % power (~ 120 mW cm^{-2}) for 5 min. This floating setup prevented the top surface of the MSDs from being activated with NHS. The MSDs were then washed once with DMSO, once with 2-propanol, and then three times with PBS under sonication. The NHS-activated MSDs were floated top side-down on a solution containing a capture probe (*i.e.,* biotin, antibody and nucleic acid) for 2 h, immobilizing the capture probes only inside the BATs as the top is not NHS-

activated and the bottom is not in contact with the solutions. After washing the MSDs three times with PBS for 1 min each, the MSDs were submerged into 50 mM 1H,1H-heptafluorobutylamine in PBS for 30 min, quenching unreacted NHS. After 3 washes for 1 min each, the functionalized MSDs were blocked with SuperBlock™ Blocking Buffer for 1 h before use.

For functionalization with biotin, MSDs were incubated in a 1 mM biotin in PBS. To vary the surface coverage of biotin on the BATs, mPEG2-amine was mixed with biotin-PEG7-amine in varying ratios while maintaining a total molarity of 1 mM for the mixture. For capture nucleic acid immobilization, amine-modified capture DNA oligonucleotides were used at concentrations of 1 μM for BAT capture efficiency measurements and at 2 μM for miR-141 detection, both prepared in PBS 10x. For antibody functionalization, MSDs were incubated with a 10 μg ml^{-1} antibody solution prepared in PBS. For quality control, one of the functionalized MSDs in a batch was fluorescently labelled and inspected under a microscope (Fig. S9b,d,f). Fluorescent labelling was performed using Streptavidin, Alexa Fluor™ 647 Conjugate (Cat. #S32357, lot # 2836838, Thermo Fisher Scientific, Waltham, MA, USA) for biotin-coated surface and nucleic acid-coated surface via the biotinylated analytes or the detection probe, and Goat anti-Mouse IgG (H+L) Cross-Adsorbed Secondary Antibody, Alexa Fluor™ 647 (Cat. #A21235, lot #2482945, Thermo Fisher Scientific, Waltham, MA, USA) for antibody-coated surfaces.

<u>SβG conjugation</u>

Streptavidin and βG were conjugated by click chemistry[37]. The βG solution was purified by anion exchange chromatography (proFIRE, Dynamic Biosensors GmbH, Munich, Germany) to remove protein aggregates[33]. 10 mg ml^{-1} streptavidin and 3 mg ml^{-1} purified βG solutions were then reacted with TCO-PEG4-NHS ester at 0.9 molar equivalents, and methyltetrazine-PEG4-NHS ester at a 15 molar equivalents, respectively, in PBS for 30 min at room temperature. Following a subsequent buffer exchange to PBS using a Zeba™ spin desalting column (Cat. #89882, lot #YK373207, Thermo Fisher Scientific, Waltham, MA, USA), the activated streptavidin and βG were incubated together overnight at 4 ºC to form SβG conjugates by click chemistry. The solution was then filtered using Amicon® Ultra Centrifugal Filter, 100 kDa MWCO (Cat. #UFC5100, lot #0000280113, Sigma-Aldrich, Oakville, ON, Canada) to remove free streptavidin. The purified SβG solution in PBS was mixed with glycerol to a final concentration of 50% (v/v), then supplemented with 5 mM $MgCl_2$ and stored at –20 °C. SβG concentration was

evaluated by absorbance at 280 nm measured with a NanoDrop™ 1000 Spectrophotometer (Thermo Scientific, Waltham, MA USA). The molecular ratio of streptavidin to βG in the conjugated SβG was analysed by performing SDS-PAGE and native PAGE using Mini-PROTEAN® TGX™ precast gels (Cat. #4561096DC, lot #64612653, Bio-Rad, Hercules, CA, USA). It was found that on average, the SβG conjugate contained one βG unit conjugated to 1.23 streptavidin molecules, with an average molecular weight of 530 kDa. Based on Poisson statistics, 29.2% molecules lack streptavidin and consist solely of βG, which was accounted for in the analysis, while free streptavidin had been removed previously via filtration.

Biotinylation of Influenza A nucleoprotein detection antibody

The detection antibody for Influenza A nucleoprotein (Anti-H7N9 Nucleoprotein) was biotinylated in-house using the EZ-Link™ NHS-PEG4 biotinylation kit (Cat. #21455, lot # YF376472, Thermo Fisher Scientific, Waltham, MA, USA). NHS-PEG4-biotin was prepared at 10 mM in water and added to the antibody solution at a 50-fold molar excess. After 30 min incubation at room temperature, the mixture was buffer-exchanged into PBS using a Zeba™ spin desalting column. The degree of biotinylation was quantified using the standard HABA (4'-hydroxyazobenzene-2-carboxylic acid)/avidin assay. The biotinylated antibody solution was mixed 1:10 into the standard HABA/avidin assay solution containing 0.5 mg/mL avidin (Cat. #1862423, lot #XJ364134, Thermo Fisher Scientific, Waltham, MA, USA) and 300 μM HABA (Cat. #1854180, lot #YB364762, Thermo Fisher Scientific, Waltham, MA, USA) in PBS, and absorbance at 500 nm was then measured using NanoDrop™ 1000 spectrophotometer for quantification of biotin.

Measurement of capture probe surface density and kinetic constants

The surface density of biotin was measured using the HABA/avidin assay. The pristine and biotin-functionalized MSDs were each placed in 10 μL of the standard HABA/avidin assay solution, and absorbances of the solution at 500 nm were measured using NanoDrop™ 1000 spectrophotometer to evaluate the depletion of the avidin-HABA complex caused by the surface-immobilized biotin. Considering that the surface binding of each avidin molecule with the tetravalent binding capacity to HABA results in the loss of four HABA molecules in the solution, the estimated biotin density was corrected by dividing by a factor of four. The surface density of biotin was modulated by ratiometric incorporation of polyethylene glycol (PEG) spacers. To

determine the surface densities of antibodies, 200 μL of 10 μg mL^{-1} antibody solutions were incubated with and without an NHS-activated MSD under the same conditions used for the MSD functionalization. Then, concentrations of the antibody solutions were quantified using the microBCA protein assay kit (Cat. #23235, lot #YC366116, Thermo Fisher Scientific, Waltham, MA, USA) measuring absorbance at 562 nm with NanoDrop™ 1000 spectrophotometer. The difference in concentration between the two conditions was attributed to antibody immobilization on the BAT surface. The surface density of the capture nucleic acid was measured by depletion of fluorescent reporter DNA oligonucleotide complementary to the capture probe. The pristine and functionalized MSDs were incubated in 10 μL of a 24 nM complementary fluorescent probe (5'-/56-FAM/TGG TGA TGC GT/36-FAM/ -3', Integrated DNA Technologies, Coralville, IA, USA) in 10 mM Tris, pH 8.0, 1 M NaCl and 0.05% Tween 20 in nuclease-free water (TNT) for 3 min. Reporter concentrations in solution were measured using NanoDrop™ 3300 Fluorospectrometer (Thermo Scientific, Waltham, MA, USA). The concentration difference between the two conditions was attributed to the surface-immobilized capture nucleic acid.

While kinetic constants of biotin and nucleic acid capture probes were obtained from the literature[38,39], those of anti-streptavidin and anti-βG antibodies were measured by a standard SPR protocol on Sierra SPR®-24 Pro (Bruker, Billerica, MA, USA) with high-capacity amine sensors (Cat. #1814895, lot #0823.a, Bruker, Billerica, MA, USA). The gold surface coated with carboxymethylated dextran was activated by injecting 400 mM EDC (Cat. #03449, lot #BCCG7233, Sigma-Aldrich, Oakville, ON, Canada) and 50 mM NHS (Cat. #24500, lot #XA342567, Thermo Fisher Scientific, Waltham, MA, USA) in water at 5 μL min^{-1} for 420 s, followed by washing with PBS with 0.05% Tween-20 (PBST) at 5 μL min^{-1} for 60 s. Antibodies (50 μg ml^{-1} in 10 mM acetate, pH 5) were immobilized by injection at 5 μL min^{-1} for 600 s. Unreacted NHS esters were quenched by 1M ethanolamine (pH 8.5; Cat. #E9508, lot #SLBR1870V, Sigma-Aldrich, Oakville, ON, Canada) in water at 10 μL min^{-1} for 420 s, followed by a final PBST wash at 10 μL min^{-1} for 240 s. For kinetic analysis, SβG in PBST was injected at 25 μL min^{-1} for 480 s (association), followed by PBST alone at 25 μL min^{-1} for 1,000 s (dissociation). Sensorgrams were analysed using standard kinetic modelling to extract k_{on} and k_{off} values.

MSD test experimental setup

As detailed in Fig. S1, an MSD was mounted on a PDMS housing cast against a 3D-printed mould. A programmable multi-channel syringe pump (Base module cat. #NEM-B004-01 B, dosing unit cat. #NEM-B002-02 B, Cetoni GmbH, Korbussen, Germany) connected to the PDMS housings via Tygon E-3603 tubing drove the sequential flow for MSD test, while the sample and the reagents were manually pipetted on the MSDs. The MSDs were then submerged into a bath filled with Fluorinert™ FC-40 for 1-min signal generation from 100 μM RGP in PBS with 1 mM $MgCl_2$. The MSDs were placed on an empty petri dish and imaged on an inverted fluorescence microscope (Ti2, Nikon, Melville, NY, USA) equipped with an sCMOS camera (Prime 95B, Teledyne Photometrics, Tucson, AZ, USA) using a 10× objective. Images were acquired with an exposure time of 200 ms. The images were processed using MATLAB with an in-house code (Available at https://github.com/junckerlab/MSD-readout) to identify negative ('0') and positive ('1') BATs, calculate the fraction of positive to total BATs f_{pos}, and convert f_{pos} to the average number of enzymes per BAT (AEB). At an AEB < 0.5, considering Poisson statistics, the images were digitally processed and f_{pos} was converted to AEB by

$$\mathrm{AEB} = -\ln(1 - f_{\mathrm{pos}}) \tag{3}$$

At an AEB > 0.5, the AEB was obtained in an analogue manner as follows.

$$\mathrm{AEB} = \frac{\bar{I}_{\mathrm{BAT}}}{\bar{I}_{\mathrm{Single}}} \tag{4}$$

where $\bar{I}_{\mathrm{single}}$ is an average intensity of single BATs obtained from MSDs at an 0.1 < AEB < 0.5 and $\bar{I}_{\mathrm{BAT}}$ is an average intensity of BATs in images under process. At least 100,000 BATs (*i.e.*, >20% of the total BATs) were analysed for a statistically robust evaluation of AEBs.

One-step MSD test using SβG as the "analyte-detection probe-enzyme"

For one-step MSD test for BAT efficiency measurement, 200 μL SβG samples in PBST were flowed through MSDs. Three different concentrations, 2 fM, 400 aM, and 80 aM of SβG, were loaded for biotin- and antibody-functionalized MSDs. For anti-βG antibody, molarity of the SβG conjugate was adjusted to include βG content, as the anti-βG antibody captures both βG with and without streptavidin. For nucleic acid-functionalized MSDs, the biotinylated DNA nucleotide analytes, including full complementarity and double mismatch, were pre-coupled with SβG, by spiking SβG at a 200-fold excess (2 nM) into 10 pM analyte. Following 10 min incubation at room

temperature, the SβG-oligonucleotide analyte complexes were diluted to final concentrations of 2 fM, 400 aM and 80 aM. After the sample flow, the MSD was then washed with PBST for 1 min (400 pL at $\bar{U}$ = 133 μm s^{-1}; Q = 6.67 pL s^{-1} per BAT) and filled with 100 μM RGP in PBS with 1 mM $MgCl_2$ for 1 min (400 pL at $\bar{U}$ = 133 μm s^{-1}; Q = 6.67 pL s^{-1} per BAT). Following 1 min signal generation in an FC-40 oil bath, the MSD was imaged under a microscope and BAT efficiency was obtained as a ratio of the experimental to theoretical AEB. The binding curve for SβG was obtained with 200 μL of SβG standards in SuperBlock™ Blocking Buffer flowed for 1 min (400 pL at $\bar{U}$ = 133 μm s^{-1}; Q = 6.67 pL s^{-1} per BAT) and the same downstream workflow as the BAT efficiency measurement. The limit of detection (LOD) was defined as the concentration yielding an AEB equal to the mean of the zero-concentration sample plus three standard deviations, determined from experimental data and theoretical Poisson noise, with the higher value selected.

Sandwich MSD test for IL-4 and Influenza A Virus nucleoprotein

For MSD test for IL-4 and Influenza A nucleoprotein, 200 μL standard samples prepared in SuperBlock™ Blocking Buffer were flowed through MSDs for 1 min (400 pL at $\bar{U}$ = 133 μm s^{-1}; Q = 6.67 pL s^{-1} per BAT), followed by 10 nM detection antibody in SuperBlock™ Blocking Buffer for 1 min (200 pL at $\bar{U}$ = 66.3 μm s^{-1}; Q = 3.33 pL s^{-1} per BAT). After a wash with PBST for 15 s (400 pL at $\bar{U}$ = 531 μm s^{-1}; Q = 26.67 pL s^{-1} per BAT), 4 pM SβG in SuperBlock™ Blocking Buffer was flowed for 1 min (200 pL at $\bar{U}$ = 66.3 μm s^{-1}; Q = 3.33 pL s^{-1} per BAT). Following a brief wash with PBS for 15 s (400 pL at $\bar{U}$ = 531 μm s^{-1}; Q = 26.67 pL s^{-1} per BAT), the MSDs were filled with 100 μM RGP in PBS with 1 mM $MgCl_2$ for 30 s (400 pL at $\bar{U}$ = 265 μm s^{-1}; Q = 13.33 pL s^{-1} per BAT). After signal generation in an FC-40 oil bath for 1 min, the MSDs were imaged under a microscope for AEB readout. All LODs were defined as the concentrations yielding an AEB three standard deviations above the mean AEB of the zero-concentration sample.

ELISA for IL-4 and Influenza A virus nucleoprotein

Standard ELISA for IL-4 and Influenza A nucleoprotein were performed on Nunc MaxiSorp 96-well plates. Wells were coated with 2 μg mL^{-1} capture antibody in 50 mM carbonate buffer, pH 9.4 overnight at 4 °C. The wells were washed five times with PBST, each wash 1 min, and blocked with 3% BSA in PBST for 2 h at room temperature. Standard samples were prepared in PBST containing 1% BSA and added to the wells for 2 h incubation at room temperature,

followed by five 1 min washes with PBST. Detection antibodies were diluted in PBST with 1% BSA to 2 μg mL^{-1} for IL-4 and 1 μg mL^{-1} for Influenza A nucleoprotein and incubated for 1 h at room temperature. The wells were again washed five times with PBST, followed by incubation with streptavidin-HRP diluted 1:50,000 in PBST with 1% BSA for 30 min at room temperature. After a final series of five 1 min washes, TMB substrate was added for signal generation at room temperature and the reaction was stopped using 0.16M sulfuric acid after 10 min. Absorbance was measured at 450 nm using a F129013 Safire plate reader (Tecan, Männedorf, Switzerland). All LODs were defined as the concentrations yielding an AEB three standard deviations above the mean AEB of the zero-concentration sample.

Sandwich MSD test for microRNA-141

For MSD test for miR-141, 200–5000μL miR-141 standard samples prepared in TNT were flowed through MSDs for 1–25 min (400–10,000 pL at $\bar{U}$ = 133 μm s^{-1}; Q = 6.67 pL s^{-1} per BAT). Then, 10 nM detection oligonucleotide in TNT was flowed through MSDs for 1 min (200 pL at $\bar{U}$ = 66.3 μm s^{-1}; Q = 3.33 pL s^{-1} per BAT). After a wash with TNT for 15 s (400 pL at $\bar{U}$ = 531 μm s^{-1}; Q = 26.67 pL s^{-1} per BAT), 4 pM SβG in SuperBlock™ Blocking Buffer was flowed for 1 min (200 pL at $\bar{U}$ = 66.3 μm s^{-1}; Q = 3.33 pL s^{-1} per BAT). Following a brief wash with PBS for 15 s (400 pL at $\bar{U}$ = 531 μm s^{-1}; Q = 26.67 pL s^{-1} per BAT), the MSDs were filled with 100 μM RGP in PBS with 1 mM $MgCl_2$ for 30 s (400 pL at $\bar{U}$ = 265 μm s^{-1}; Q = 13.33 pL s^{-1} per BAT). After signal generation in an FC-40 oil bath for 1 min, the MSDs were imaged under a microscope for AEB readout. The LOD was defined as the concentrations yielding an AEB three standard deviations above the mean AEB of the zero-concentration sample.

RT-qPCR and RT-ddPCR for microRNA-141

Reverse transcription (RT) was carried out using a stem-loop RT primer to generate elongated cDNA from the 22-nt miR-141. Briefly, 5 μL of miR-141 standard solution was added into a 10 μL RT reaction mix containing the TaqMan™ RT primer. The RT reaction was conducted on Biometra T-Gradient thermocycler (Analytik Jena, Germany) under the thermal cycling conditions as follows: 30 min at 16 °C (annealing), 30 min at 42 °C (reverse transcription), and 5 min at 85 °C (enzyme inactivation) and stored at -20°C (long term storage). Real-time PCR of the miR-141 RT product was performed following the manufacturer's standard procedure. 0.67 μL of the RT product was added to 9.34 μL of the PCR reaction mix containing PCR primers and

TaqMan™ probe. Reactions were initiated with enzyme activation at 95 °C for 10 min, followed by 40 amplification cycles of 95 °C for 15 s (denaturation) and 60 °C for 60 s (annealing/extension). Thermal cycling and real-time fluorescence recording were performed using a CFX Connect real time PCR machine (Bio-Rad, Hercules, CA, USA). Ct value from the no template control was used to set the Ct cutoff. For ddPCR, 1.34 µL of the miR-141 RT product was added to 18.66 µL of ddPCR mix and loaded into the droplet generator cartridge of a QX200 Droplet Generator (BioRad, USA) along with 65 µL of ddPCR droplet generation oil to generate 37.5 µL of droplets. PCR reaction was initiated at 95 °C for 10 min, followed by 35 amplification cycles of 95 °C for 15 s and 60 °C for 60 s using C1000 Touch Thermal Cycler (Bio-Rad, Hercules, CA, USA). Signal readout was carried out on a QX200 Droplet Reader (Bio-Rad, Hercules, CA, USA).

Influenza A nasopharyngeal sample analysis

15 influenza A-positive and 15 negative nasopharyngeal swab samples were collected by American Blood Services DBA under an appropriate institutional review board (IRB) protocol (IRB approval ID: 45469786) and purchased. The lysis of influenza A nucleoprotein was performed by mixing the nasopharyngeal swab samples in universal transport medium (UTM) with lysis buffers at a ratio of 1:1:8 (buffer A:buffer B:sample) and incubated for 5 min at room temperature. Buffer A contained 500 mM Tris, 150 mM NaCl, 10 mM DTT, 20 mM EDTA, 10× protease inhibitor cocktail, 1 mg ml^{-1} RNase A, and 50% (v/v) glycerol in water and buffer B consisted of 10% (v/v) Triton X-100 and 150 mM NaCl in water. To perform rapid tests, 85 µL of the processed sample was loaded on Influenza AB + COVID-19 Antigen – 3 in 1 Test. At 15 min, the rapid tests were imaged, and the intensities of the test lines relative to the background were quantified using ImageJ software. To perform MSD test, the processed sample was diluted 1:5 in SuperBlock™ Blocking Buffer, and 200 µL of the diluted sample was analysed based on the detection method described above.

References

1 Squires, T. M., Messinger, R. J. & Manalis, S. R. Making it stick: convection, reaction and diffusion in surface-based biosensors. *Nat. Biotechnol.* **26**, 417-426 (2008).

2 Cesaro-Tadic, S. *et al.* High-sensitivity miniaturized immunoassays for tumor necrosis factor α using microfluidic systems. *Lab Chip* **4**, 563-569 (2004).

3 Yafia, M. *et al.* Microfluidic chain reaction of structurally programmed capillary flow events. *Nature* **605**, 464-469 (2022).

4 Elshal, M. F. & McCoy, J. P. Multiplex bead array assays: Performance evaluation and comparison of sensitivity to ELISA. *Methods* **38**, 317-323 (2006).

5 Dagher, M. *et al.* nELISA: a high-throughput, high-plex platform enables quantitative profiling of the inflammatory secretome. *Nat. Methods* **22**, 2375-2385 (2025).

6 Mullis, K. B. & Faloona, F. A. in *Methods Enzymol.* Vol. 155 335-350 (Academic Press, 1987).

7 Hindson, B. J. *et al.* High-Throughput Droplet Digital PCR System for Absolute Quantitation of DNA Copy Number. *Anal. Chem.* **83**, 8604-8610 (2011).

8 Zhao, Y., Chen, F., Li, Q., Wang, L. & Fan, C. Isothermal Amplification of Nucleic Acids. *Chem. Rev.* **115**, 12491-12545 (2015).

9 Shen, F. *et al.* Digital Isothermal Quantification of Nucleic Acids via Simultaneous Chemical Initiation of Recombinase Polymerase Amplification Reactions on SlipChip. *Anal. Chem.* **83**, 3533-3540 (2011).

10 Broughton, J. P. *et al.* CRISPR–Cas12-based detection of SARS-CoV-2. *Nat. Biotechnol.* **38**, 870-874 (2020).

11 Filchakova, O. *et al.* Review of COVID-19 testing and diagnostic methods. *Talanta* **244**, 123409 (2022).

12 Engvall, E. & Perlmann, P. Enzyme-linked immunosorbent assay (ELISA) quantitative assay of immunoglobulin G. *Immunochemistry* **8**, 871-874 (1971).

13 Rondelez, Y. *et al.* Microfabricated arrays of femtoliter chambers allow single molecule enzymology. *Nat. Biotechnol.* **23**, 361-365 (2005).

14 Ge, S., Liu, W., Schlappi, T. & Ismagilov, R. F. Digital, ultrasensitive, end-point protein measurements with large dynamic range via brownian trapping with drift. *J. Am. Chem. Soc.* **136**, 14662-14665 (2014).

15 Honda, S., Minagawa, Y., Noji, H. & Tabata, K. V. Multidimensional Digital Bioassay Platform Based on an Air-Sealed Femtoliter Reactor Array Device. *Anal. Chem.* **93**, 5494-5502 (2021).

16 Byrnes, S. A. *et al.* Wash-Free, Digital Immunoassay in Polydisperse Droplets. *Anal. Chem.* **92**, 3535-3543 (2020).

17 Han, B. H., Park, M., Chung, S. & Kang, J. Y. Evaporation-driven digital ELISA with micro-droplet arrays for ultrafast detection of low-abundance proteins. *Biosens. Bioelectron.* **292**, 118076 (2026).

18 Rissin, D. M. *et al.* Single-molecule enzyme-linked immunosorbent assay detects serum proteins at subfemtomolar concentrations. *Nat. Biotechnol.* **28**, 595-599 (2010).

19 Rissin, D. M. *et al.* Simultaneous Detection of Single Molecules and Singulated Ensembles of Molecules Enables Immunoassays with Broad Dynamic Range. *Anal. Chem.* **83**, 2279-2285 (2011).

20 Kan, C. W. *et al.* Digital enzyme-linked immunosorbent assays with sub-attomolar detection limits based on low numbers of capture beads combined with high efficiency bead analysis. *Lab Chip* **20**, 2122-2135 (2020).
21 Yelleswarapu, V. *et al.* Mobile platform for rapid sub–picogram-per-milliliter, multiplexed, digital droplet detection of proteins. *Proc. Natl. Acad. Sci. U.S.A.* **116**, 4489-4495 (2019).
22 Cohen, L. *et al.* Single Molecule Protein Detection with Attomolar Sensitivity Using Droplet Digital Enzyme-Linked Immunosorbent Assay. *ACS Nano* **14**, 9491-9501 (2020).
23 Wu, C., Dougan, T. J. & Walt, D. R. High-Throughput, High-Multiplex Digital Protein Detection with Attomolar Sensitivity. *ACS Nano* **16**, 1025-1035 (2022).
24 Risken, H. in *The Fokker-Planck equation: methods of solution and applications* (Springer, 1989).
25 Fullstone, G., Wood, J., Holcombe, M. & Battaglia, G. Modelling the Transport of Nanoparticles under Blood Flow using an Agent-based Approach. *Sci. Rep.* **5**, 10649 (2015).
26 Tracy, M., Cerdá, M. & Keyes, K. M. Agent-based modeling in public health: current applications and future directions. *Annu. Rev. Public Health* **39**, 77-94 (2018).
27 Bird, R. B., Stewart, W. & Lightfoot, E. N. *Transport Phenomena second edition*. (John Wiley & Sons, 2002).
28 Gervais, T. & Jensen, K. F. Mass transport and surface reactions in microfluidic systems. *Chem. Eng. Sci.* **61**, 1102-1121 (2006).
29 Brown, G. M. Heat or mass transfer in a fluid in laminar flow in a circular or flat conduit. *AIChE Journal* **6**, 179-183 (1960).
30 Deen, W. M. *Analysis of Transport Phenomena*. (OUP USA, 1998).
31 Hernández-Castro, J. A., Li, K., Meunier, A., Juncker, D. & Veres, T. Fabrication of large-area polymer microfilter membranes and their application for particle and cell enrichment. *Lab Chip* **17**, 1960-1969 (2017).
32 Meunier, A. *et al.* Gravity-based microfiltration reveals unexpected prevalence of circulating tumor cell clusters in ovarian and colorectal cancer. *Commun. Med.* **5**, 33 (2025).
33 Rissin, D. M., Gorris, H. H. & Walt, D. R. Distinct and Long-Lived Activity States of Single Enzyme Molecules. *J. Am. Chem. Soc.* **130**, 5349-5353 (2008).
34 Peng, Y. *et al.* Metal-organic framework nanosheets as building blocks for molecular sieving membranes. *Science* **346**, 1356-1359 (2014).
35 Liu, Y., Zhan, L., Qin, Z., Sackrison, J. & Bischof, J. C. Ultrasensitive and Highly Specific Lateral Flow Assays for Point-of-Care Diagnosis. *ACS Nano* **15**, 3593-3611 (2021).
36 Shafique, H. *et al.* High-resolution low-cost LCD 3D printing for microfluidics and organ-on-a-chip devices. *Lab Chip* **24**, 2774-2790 (2024).
37 Liu, F., Liang, Y. & Houk, K. N. Bioorthogonal Cycloadditions: Computational Analysis with the Distortion/Interaction Model and Predictions of Reactivities. *Acc. Chem. Res.* **50**, 2297-2308 (2017).
38 Srisa-Art, M., Dyson, E. C., deMello, A. J. & Edel, J. B. Monitoring of Real-Time Streptavidin−Biotin Binding Kinetics Using Droplet Microfluidics. *Anal. Chem.* **80**, 7063-7067 (2008).
39 Todisco, M., Ding, D. & Szostak, J. W. Transient states during the annealing of mismatched and bulged oligonucleotides. *Nucleic Acids Res.* **52**, 2174-2187 (2024).

Acknowledgements

We gratefully acknowledge M. Tabrizian and J.V.L. Nguyen for access to their SPR system and assistance, A. Kamen, J. Fulber and X. Xu for access to their ddPCR system and assistance, D. Liu at the Facility for Electron Microscopy Research of McGill University for help in microscope operation and data collection, C. Yansouni and J. Papenburg for discussions and advice, T. Gervais for proof-reading, Tri-iso and Ingevity for providing CAPA 3050 samples and Allnex for providing Ebecryl® 3708 and Tripropylene glycol diacrylate (TPGDA) samples. This research was supported by The Natural Sciences and Engineering Research Council of Canada (NSERC) Discovery Grant RGPIN-2022-05171, Canada Research Chair in Bioengineering CRC-232159, and McGill University MI4 Emergency COVID-19 Research Funding and Pathy Seed Fund Grant. G.K. acknowledges an FRQNT doctoral research scholarship and a McGill BME recruitment award. M.L.S acknowledges a Vanier Canada Graduate Scholarship and a McGill BME recruitment award.

Author contributions

Conceptualization: G.K., A.N., D.J.

Methodology: G.K., A.N., D.J.

Investigation: G.K., M.L.S.

Visualization: G.K., M.L.S.

Funding acquisition: A.N., D.J.

Supervision: D.J.

Writing – original draft: G.K., A.N., D.J.

Writing – review & editing: G.K., M.L.S., A.N., D.J.

Competing interests

G.K. and D.J. are inventors on a report of invention submitted to McGill University. All other authors declare no competing interests.

Ethics statement

Nasopharyngeal swab samples were obtained from American Blood Services DBA, Los Osos, CA, USA. According to the supplier's certification, all samples were collected under an appropriate institutional review board (IRB) protocol (IRB approval ID: 45469786).

Data availability

All data points are presented in the article and Supplementary Information. Source data will be available upon request.

Code availability

MATLAB codes for MSD image processing are available at https://github.com/junckerlab/MSD-readout.

Additional information

Supplementary Information is available for this paper. Correspondence and requests should be addressed to david.juncker@mcgill.ca.